Research in Astron. Astrophys. **2012** Vol. **12** No. **3**, 300–312
http://www.raa-journal.org *http://www.iop.org/journals/raa*

Research in Astronomy and Astrophysics

The surge-like eruption of a miniature filament *

Jia-Yan Yang[1,2], Yun-Chun Jiang[1], Dan Yang[1,3], Yi Bi[1,3], Bo Yang[1,3], Rui-Sheng Zheng[1,3] and Jun-Chao Hong[1,3]

[1] National Astronomical Observatories / Yunnan Observatory, Chinese Academy of Sciences, Kunming 650011, China; *yjy@ynao.ac.cn*
[2] Key Laboratory for the Structure and Evolution of Celestial Objects, Chinese Academy of Sciences, Kunming 650011, China
[3] Graduate University of Chinese Academy of Sciences, Beijing 100049, China

Received 2011 September 22; accepted 2011 November 11

Abstract We report on the rare eruption of a miniature Hα filament that took the form of a surge. The filament first underwent a full development within 46 min and then began to erupt 9 min later, followed by a compact, impulsive X-ray class M2.2 flare with a two-ribbon nature only at the early eruption phase. During the eruption, its top rose, whereas the two legs remained rooted in the chromosphere and showed little swelling perpendicular to the rising direction. This led to a surge-like eruption with a narrow angular extent. Similar to the recent observations for standard and blowout X-ray jets by Moore et al., we thus define it as a "blowout Hα surge." Furthermore, our observations showed that the eruption was associated with (1) a coronal mass ejection guided by a pre-existing streamer, (2) abrupt, significant, and persistent changes in the photospheric magnetic field around the filament, and (3) a sudden disappearance of a small pore. These observations thus provide evidence that a blowout surge is a small-scale version of a large-scale filament eruption in many aspects. Our observations further suggest that at least part of the Hα surges belong to blowout-type cases, and the exact distinction between the standard and blowout Hα surges is important in understanding their different origins and associated eruptive phenomena.

Key words: Sun: activity — Sun: filaments — Sun: flares — Sun: magnetic field — Sun: coronal mass ejections (CMEs)

1 INTRODUCTION

Solar filaments show some common characteristics over a broad spectrum of scales. Along the polarity inversion zone between adjacent opposite-polarity photospheric fields on the quiet Sun, miniature filaments are the small-scale analog to large-scale ones. Hermans & Martin (1986) concluded that their eruptions appear to be the counterparts of large-scale filament eruptions, which are usually associated with two-ribbon flares and coronal mass ejections (CMEs). Wang et al. (2000) showed

* Supported by the National Natural Science Foundation of China.

that miniature filaments have a mean lifetime of only 50 min, and their eruptions can take varying forms but almost all are accompanied by tiny flares, with spatial patterns very similar to two-ribbon/multiribbon flares in large-scale filament eruptions. Sakajiri et al. (2004) and Ren et al. (2008) also suggested that small- and large-scale filament eruptions have common properties. Therefore, it is reasonable to expect that some small-scale filament eruptions can also be related to CMEs (Innes et al. 2009; Schrijver 2010) and should be explained in the framework of the "standard model" for solar eruptions, in which an overlying arcade erupts, producing a flare along with an ejecting filament. However, Wang et al. (2000) showed that most miniature filaments have erupted toward nearby strong network elements, meaning that perhaps most of their mass is transported to other magnetic structures rather than ejected into the corona. Therefore, questions are naturally raised: is the mass transport along pre-existing magnetic force lines? Can small-scale filament eruptions be strong enough to escape into the heliosphere? Detailed observations of small-scale filament eruptions could help to answer these questions.

Strongly related dynamical phenomena that can be closely associated with CMEs are plasma ejections following open or far-reaching field lines, which show up as surges in Hα and jets in EUV and X-ray. Hα surges are straight or slightly curved mass ejections stretching out and away from small flares at the footpoints in the chromosphere into coronal heights (Roy 1973; Bruzek & Durrant 1977), and it is believed that they are produced by reconnections between emerging flux and ambient open or far-reaching magnetic structures (Schmieder et al. 1995; Canfield et al. 1996; Jiang et al. 2007, 2011; Madjarska et al. 2007; Chifor et al. 2008; Moreno-Insertis et al. 2008; Patsourakos et al. 2008; Pariat et al. 2010; Yang et al. 2011). Therefore, surges have quite different physical processes and scenarios from those of small filament eruptions. However, some observations have showed that both of them can be related to the same kind of eruptive phenomena, especially "narrow CMEs" with angular widths of about 15° or less and impulsive solar energetic particle (SEP) events. Gilbert et al. (2001) concluded that 15 narrow CMEs originate in regions of closed magnetic fields since they have a high association with filaments, but Dobrzycka et al. (2003) cannot definitively determine whether they originate from jets or filament eruptions. Liu (2008) showed that large jetlike/diffuse Hα surges are associated with jetlike/wide-angle CMEs. It is noted that, however, their Hα data might have inadequate spatial resolution to tell us whether the surge bases include tiny filaments or not. Meanwhile, when white-light jets can be accompanied by either EUV bright points (Paraschiv et al. 2010) or filament eruptions (Wang & Sheeley 2002), impulsive SEP events can also be closely associated with EUV and corresponding white-light jets that involve open field lines (Wang et al. 2006), as well as with motions that look like filament eruptions (Nitta et al. 2006). In order to get a clear physical picture of these eruptive phenomena, it is clear that a definitive distinction of their different origins is desired.

On the other hand, some observations indeed presented evidence that plasma ejections can be physically related with some kinds of activations or eruptions of small filaments. Chae et al. (1999) first reported that Hα surges, EUV jets, and associated microflares were preceded by a small filament eruption. Zuccarello et al. (2007) showed that the destabilization and disappearance of a small short-lived filament followed two Hα surges pouring sequentially from part of the filament body. Consistent with previous results (Yamauchi et al. 2005), in particular, Moore et al. (2010) found that in the polar coronal holes (CHs) two-thirds of X-ray jets are standard ones that fit the standard reconnection picture for coronal jets, while the other one-third are so-called blowout jets in which the jet-base magnetic arch, often carrying a filament, undergoes a miniature version of the blowout eruptions that produce major CMEs. Similarly, Raouafi et al. (2010) showed that coronal jets can erupt from coronal micro-sigmoids, and Nisticò et al. (2009) also found some micro-CME-type jet events resembling the classical CMEs. Quite recently, Hong et al. (2011) and Zheng et al. (2011) indeed showed that miniature filament eruptions can lead to blowout jets and small CMEs. Therefore, at least part of plasma ejections have originated from small-scale filament eruptions, and high-resolution observations are needed to understand the possible relation between them or to dis-

tinguish them from each other. Similar to the cases in large-scale filament eruptions, in addition, a few examples clearly suggested that the flux emergence and cancelation play an important role in disturbing small filaments (Hermans & Martin 1986; Sakajiri et al. 2004; Ren et al. 2008; Hong et al. 2011). It thus appears that small filament eruptions have similar exterior driving agents to those of surges or jets (Yoshimura et al. 2003; Jiang et al. 2007). Like the cases occurring in some major flares (Wang et al. 2002b; Sudol & Harvey 2005; Petrie & Sudol 2010; Wang & Liu 2010), an abrupt, significant, and persistent change in the photospheric magnetic field was also found in a CME-associated Hα mass ejecta event (Uddin et al. 2004; Li et al. 2005). Therefore, it is probable that such an extreme change could also take place in small-scale filament eruptions, and detailed magnetic field observations could help in verifying this possibility.

On 2001 March 27, a surge-shaped eruption occurred in AR 9401 (N21°, E33°), and was associated with a compact impulsive flare, a CME, and especially, a sudden and permanent change of the magnetic field and the disappearance of a small pore. High-resolution Hα observations from Big Bear Solar Observatory (BBSO) help us to find that it was in fact a small-scale filament eruption. Due to the short lifetime of the filament, the complete process from its formation to eruption was observed, hence providing us with the opportunity to investigate why the eruption took a surge form and its relationship with the CME and photospheric field activity.

2 OBSERVATIONS

The eruption was well covered by full-disk Hα line-center observations from BBSO, with a 1-min image cadence and a pixel size of roughly $1''$. The magnetic field configuration of the eruptive region was examined using full-disk magnetograms and continuum intensity images from the Michelson Doppler Imager (MDI; Scherrer et al. 1995) aboard the *Solar and Heliospheric Observatory* (*SOHO*). The magnetograms have a 1-min cadence and a pixel size of $2''$, while continuum images only have a 96-min cadence. The MDI data are obtained from nine filtergrams taken in five different positions in the Ni I 6768 Å absorption line in right- and left-circularly polarized light, and the continuum intensity is estimated from a filtergram averaging narrowband signals from both sides outside the line. The full-disk BBSO to MDI co-alignment was done by fitting the solar limbs, with an accuracy of about $2''$.

This eruption was also examined by using full-disk EUV observations from the Extreme Ultraviolet Telescope (EIT; Delaboudinière et al. 1995) on *SOHO*. The 12-min cadence 195 Å images were obtained for the study with a pixel resolution of $2.6''$. To identify the associated CME, we used the C2 and C3 white-light coronagraph data from the Large Angle and Spectrometric Coronagraphs (LASCO; Brueckner et al. 1995) on *SOHO*, as well as the CME height-time data that are available in the LASCO Web site. Finally, we used soft X-ray light curves observed by the *Geostationary Operational Environmental Satellite* (*GOES*) to track the time of the flare.

3 RESULTS

The surge-like solar eruption was accompanied by a flare of Hα importance 1N and X-ray class M2.2, for which *GOES* recorded its start, peak, and end times around 16:25, 16:30, and 16:32 UT, respectively.

Figure 1 presents BBSO Hα line-center images to show the morphological evolution of the event. To aid matching, an MDI magnetogram is given in the first frame. The Hα flare appeared compact. It started to brighten slightly prior to the *GOES* flare start time, increased in size, flared through the period of the *GOES* flare, quickly faded away, and finally disappeared after about 16:40 UT. Therefore, the flare behaved as a compact, impulsive case with a total duration of only 7 min. A striking characteristic of the event is that a surge-like mass ejection occurred in the course of the flare, which showed up as extended linear structures with much larger size than that of the compact flare patch. When the *GOES* flare started (16:25 UT), a single bright structure (indicated by the white

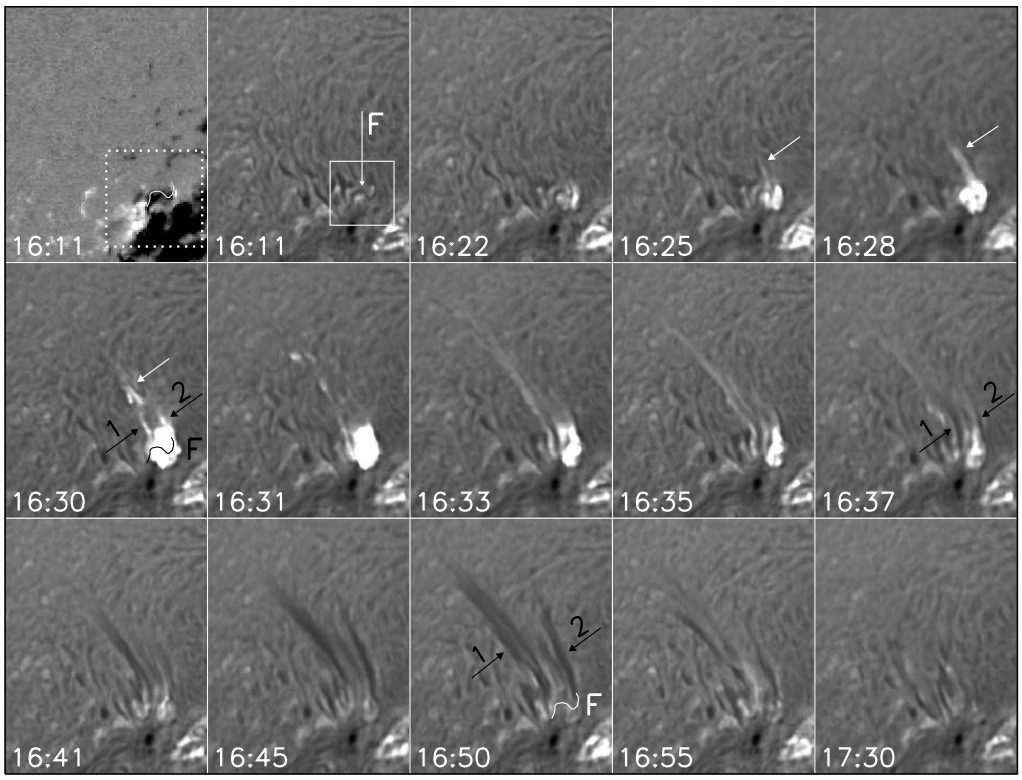

Fig. 1 BBSO Hα line-centered images showing the evolution of the event. The first panel is an MDI magnetogram. Accompanied by a compact flare, the surge-like mass ejection with two leg-shaped features, '1' and '2,' originated from the eruption of a tiny filament, 'F,' at its base. The outlines of F's axis determined from the 16:11 UT Hα image are plotted as solid curves. The cases of '1' and '2,' indicated by the two black arrows in the 16:30 UT image, are bright 1 and bright 2 respectively, while '1' and '2,' also indicated by the two black arrows in the 16:37 UT and 16:50 UT images, are dark 1 and dark 2 respectively. The field-of-view (FOV) is $190'' \times 240''$. The solid/dotted box indicates the FOV of Fig. 2/Fig. 6.

arrow) was first ejected from the flare patch. By the *GOES* flare peak time (16:30 UT), however, the bright structure clearly evolved into a narrow bright loop (indicated by the white arrow) with two legs, '1' and '2' (indicated by the two black arrows). The leg 2 quickly became ambiguous, while the leg 1 largely lengthened towards the northeastern direction and showed a slightly curved triangular shape, thus remarkably being displayed as a surge (Kurokawa & Kawai 1993). Beginning at about 16:37 UT after the *GOES* flare ended, two dark components, also labeled as '1' and '2,' grew nearly along the same trajectories as the two bright legs (indicated by the two black arrows). When the dark 1 gradually grew to occupy the whole path of the bright 1, the dark 2 underwent a larger development than that of the bright one. It is possible that the dark components were caused by the cooling of earlier, brighter components since they were co-spatial and shared the same paths. Then the two dark components gradually faded away and became invisible after about 16:55 UT.

Since Hα surges can be entirely in emission and dark surges can be preceded by bright ones (Svestka et al. 1990), at first glance, the above morphological characteristic of the eruption gives us an impression that this was a surge activity consisting of both bright and dark components, which

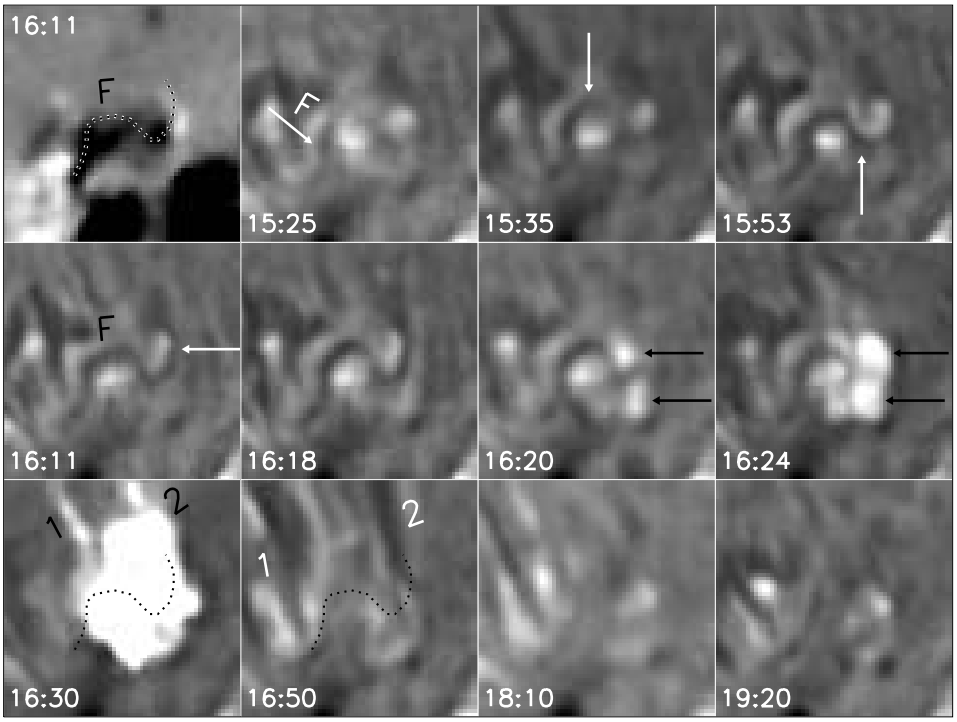

Fig. 2 Close-up view of F in BBSO Hα images. The first panel is an MDI magnetogram. The white arrows indicate that F grew toward the west, and the black arrows indicate the initial brightenings of the flare showing its two-ribbon nature. The outlines of F's axis as in Fig. 1 are plotted, and its two legs are marked as '1' and '2.' The FOV is $60'' \times 60''$.

occurred one after another, first bright then dark. Thanks to the high-resolution Hα observations, however, we can remark by chance that there existed a tiny filament, 'F,' at the flare site before the eruption (see the 16:11 UT frame in Fig. 1). Moreover, we found that the legs 1 and 2 coincided with those of the erupting F (see the 16:30 and 16:50 UT frames in Fig. 1). Therefore, it is very likely that the surge-like ejection was coming from the F eruption. This motivates us to further investigate the F evolution in detail. Fortunately, BBSO's observations covered the key process of the F formation and eruption. This is shown by the close-up view of F in Figure 2. When BBSO's observations started at 15:25 UT, F was seen as a very small dark feature nearly residing above a magnetic polarity reversal boundary between an adjacent opposite-polarity photospheric field. In less than 1 hr, it grew toward the west with a curved path along the polarity reversal boundary (indicated by the white arrows), and by about 16:11 UT, reached its maximum extent with a length of about 3.86×10^4 km, about two times as long as miniature filaments with an average projected length of 1.9×10^4 km (Wang et al. 2000). Therefore, F was a somewhat larger miniature filament. It is of interest to note that at this time it exhibited an inverse-S shape, consistent with the preferential pattern of a dextral filament in the northern hemisphere (Pevtsov et al. 2003). However, soon afterwards, its westernmost part began to disappear and two bright patches appeared at its two sides just before the *GOES* flare started (indicated by the black arrows in the 16:20 and 16:24 UT images in Fig. 2). This is consistent with Kahler et al. (1988) that filaments began to erupt before the starting times of associated flares.

Finally, the entire F quickly became invisible along with the area increase of the flare. Since F did not recover from such a disappearance in the following 2h even when the flare completely

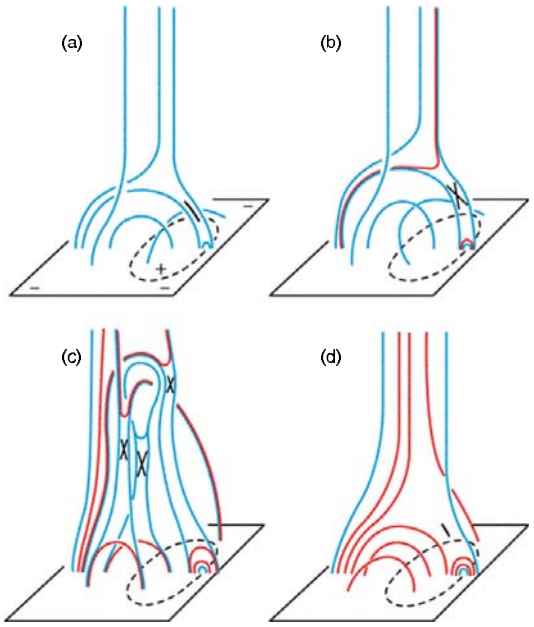

Fig. 3 Schematic depiction of the production of a blowout coronal jet from Moore et al. (2010). Reproduced by permission of the AAS. Only a few representative lines are drawn. Red field lines are those that have been reconnected with reconnection-heated X-ray plasma on them, while blue field lines either have not yet been reconnected or will not be reconnected (*color online*). (a) Pre-eruptive magnetic field setup. A bipolar arch emerges in a negative-polarity CH field. The dashed oval is the neutral line around the positive flux of the emerging arch, the short black curve represents the current sheet, and the field line arching low along the neutral line in the middle of the base arch indicates that the core field of the arch is extremely sheared. (b) Magnetic reconnection (marked by the X) at the location of the current sheet produces the small red loop on the west side and the red field line anchored on the east side. If the emerging arch has no sheared or twisted core field, the latter forms a standard X-ray jet and then the eruption would end shortly after this time. (c) If the core field of the emerging arch is strongly sheared and twisted, its blowout eruption leads to reconnection at several locations (marked by the Xs) that produces a blowout jet with a curtain-like structure, a red flare arcade in the east of the neutral line, and an additional brightening and growth of the loop in the west. (d) At the decay phase, the X-ray jet narrows and the entire field structure begins to relax down to the configuration of (a).

faded away, we can conclude that it really underwent an overall violent eruption rather than was simply covered and obscured by the flare emission. It is noted that there were some filament-like dark features around F that were disturbed or even partially disappeared during the eruption. By carefully examining the eruption process, however, it is found that the legs 1 and 2 did not belong to them but were just the two legs of the erupting F. This is clearly indicated by the 16:30 and 16:50 UT Hα images, where the outlines of F's axis at 16:11 UT were superposed as dashed lines. Therefore, the surge-like ejection had simply originated from the F eruption at its base in a narrow way: when its two ends were fixed in the chromosphere, its top quickly lifted up but its axis only had a little swelling or expansion perpendicular to the rising direction (also see Fig. 1). This means that they were the same phenomenon, i.e. a filament eruption taking the form of a surge (Nisticò et al. 2009; Moore et al. 2010; Raouafi et al. 2010; Hong et al. 2011).

The schematic shown in Figure 3, a copy of figure 10 in Moore et al. (2010), depicts the scenario for the productions of both standard and blowout jets. The magnetic field setup for both cases is the same as that of a compact, low-arching bipolar field which emerges into a pre-existing, high-reaching, unipolar CH field with negative polarity, thus forming a neutral line surrounding the positive base of the emerging bipole, as well as a current sheet at the interface between the ambient field and its positive-leg (Fig. 3(a)). If the emerging-arch field has no appreciable shear or twist in it, magnetic reconnection at the current sheet creates a miniature-flare-arcade bright point over the west-side neutral line below the reconnection X-point, as well as a standard X-ray jet with a single-strand spire whipping out of the top side of the reconnection X-point (Fig. 3(b)). The eruption process then finishes, the field relaxes down to the Figure 3(a) configuration and the emerging arch to the east of the new reconnection loop in Figure 3(b) remains stable. In the blowout jet case, however, an essential difference is that the core field of the emerging bipolar arch is so strongly sheared and twisted that it often shows up as a small filament and has enough free energy to drive a blowout of the arch: the emerging arch becomes destabilized by the earlier dynamics and thus triggers a blowout eruption of the sheared core field as in a filament eruption. As depicted in Figure 3(c), reconnection then occurs at three places that can result in a blowout X-ray jet with a multi-stranded curtain-like appearance (see Moore et al. 2010 for details of the blowout jet eruption process). Significantly, the blowout jet has a substantially larger horizontal size span than that of the standard jet.

Finally, the jet narrows and the field configuration relaxes down to the initial state of Figure 3(a) (Fig. 3(d)). It is difficult to make a one-to-one comparison between the above scenario and our event because no soft X-ray or high-resolution EUV imaging observations are available and the magnetic field environment is also different from that described by Moore et al. (2010) in terms of CHs. However, two factors make us believe that our Hα surge was clearly not a standard one. One is that it originated from the small F eruption, and the other is that its 1 and 2 components quite resembled the curtain-like blowout jet rather than the single-strand spire of Moore et al. (2010). Therefore, we can introduce a new term and call it a "blowout Hα surge." It is interesting to note that the 1 and 2 features in our event were very similar to a pair of thin ejections at the leg locations of a spicule-associated blowout jet from an eruption of relatively cool material in the event shown by Sterling et al. (2010). Taking 16:20 UT as the start time of the F eruption, F had a lifetime of about 55 min from its first formation (15:25 UT) through the eruption. This was very consistent with the 50-min mean lifetime of miniature erupting filaments given by Wang et al. (2000). Similar to a case studied by Sakajiri et al. (2004), in which a miniature filament erupted 25 min after its first formation, we find that there was an interval of only 9 min between the F eruption's start and its full development (16:11 UT). It is clear that the flare was preceded by such an eruption. Although the flare at the main phase was too compact to discern its two ribbons and separating motion (possibly due to the small size of F), similar to the situation in compact flares observed by Tang (1985), the small Hα brightenings at the initial F eruption phase clearly showed a two-ribbon nature. Consistent with some previous observations (Wang et al. 2000; Sakajiri et al. 2004; Ren et al. 2008; Hong et al. 2011), therefore, we believe that the F eruption was a small-scale version of an active-region or a quiet-region large-scale filament eruption and the flare was a direct result of such a small-scale eruption.

The eruption can be traced going beyond the northeast limb in EIT observations, and was closely associated with a CME observed by LASCO. This is quite obvious in the EIT 195 Å and LASCO C2 images presented in Figure 4. At 16:35 UT, although there was a thick, nearly straight, jet-shaped bright EUV feature responding to the Hα surge-like bright structure (see Fig. 1) on the solar disk (included in the black box), the top part of the erupting F had indeed ejected beyond the solar limb and showed a curved loop-like shape (indicated by the black arrow). It can still be clearly discernible at 16:47 UT but then sprayed out of the field-of-view (FOV) of EIT after 16:59 UT. Therefore, the EIT observation further confirmed that this was a filament eruption event. The associated CME first appeared in the LASCO C2 FOV at 17:06 UT as a ragged ejection in the northeastern direction that traveled along a thin streamer. It had a width of 66° and a central position angle (P.A.) of 46°. As

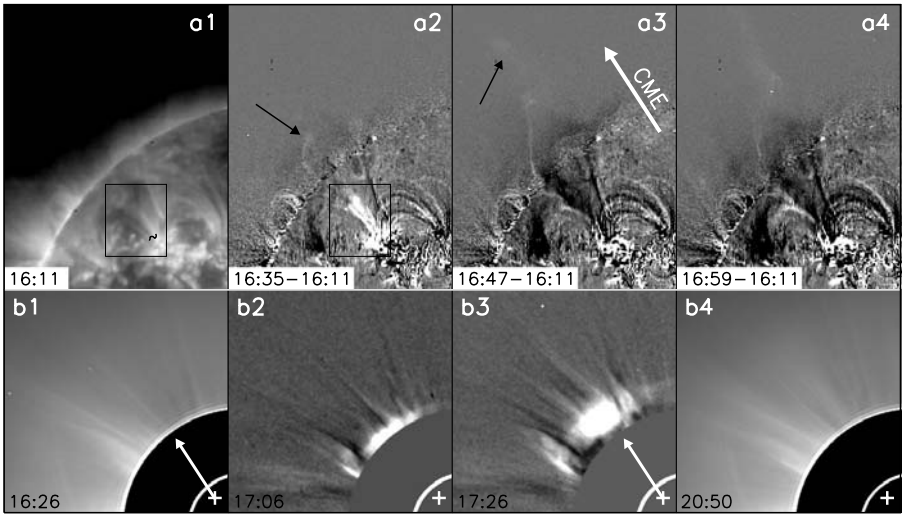

Fig. 4 EIT 195 Å (panels a1–a4) and LASCO C2 (panels b1–b4) images. Panels a1, b1, and b4 are original images, a2–a4 are EIT 195 Å fixed-base difference images obtained by subtracting a pre-flare image (a1), and b2–b3 are C2 running difference images. The black arrows indicate the erupting F, and the white arrows the eruptive direction of the CME. The outlines of F's axis as in Fig. 1 are also plotted in a1, and the plus signs mark the pre-eruptive F location. The FOV for a1–a4 is $810'' \times 1030''$, and the black boxes indicate the FOV of Fig. 1.

indicated by the white arrows, the CME's eruption direction determined from the central P.A. was along the streamer and consistent with that of the erupting F. It is noteworthy that the streamer was only slightly altered after the passage of the CME (see panels b1 and b4), which was similar to the cases of streamer-puff and over-and-out CMEs recently studied by Bemporad et al. (2005), Moore & Sterling (2007), and Jiang et al. (2009). The height-time (H-T) plot of the CME front at P.A. 38° is shown in Figure 5. By applying second-order polynomial fitting, back extrapolation of the CME front from the H-T plots to the eruptive location yields an estimate of the CME onset time near 16:17 UT, which is very close to the start time of the F eruption at 16:20 UT, as well as the start time of the flare at 16:25 UT. The spatial and temporal consistencies strongly suggest that the CME initiation was closely related to the F eruption. In addition, the application of first- and second-order polynomial fitting to the H-T points gives an average speed of 342 km s^{-1} and an acceleration of -6.2 m s^{-2}. These parameters showed that the CME was a slow one, consistent with the results showing that slow CMEs are more often found associated with filament eruptions (Sheeley et al. 1999; St. Cyr et al. 2000). It is noted that the CME front speed is very close to the average F speed of about 344 km s^{-1} estimated from 16:20 to 16:47 UT, and two H-T points of the erupting F at 16:35 and 16:47 UT plotted in Figure 5 are also close to the extrapolated curves of the CME front, implying the tight relationship between the F eruption and the CME. From 16:25 to 16:31 UT, however, we can exactly determine the top sites of the erupting F in Hα observations (see Fig. 1), and an average speed (acceleration) of about 151.8 km s^{-1} (1.4 m s^{-2}) is given. In accordance with the result of Zhang et al. (2001), these values indicate that F possibly underwent a large acceleration at its early eruption phase. As compared with the very small F size, however, we would like to point out that the CME had a much larger scale. Therefore, the F eruption and the Hα surge might only serve as a trigger and occupy a small part of the CME. Further observations are necessary to clarify such possibility.

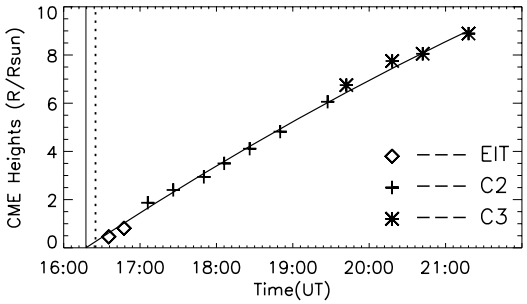

Fig. 5 Heights of the CME front as a function of time, and the back extrapolations by the use of second-order polynomial fitting. The vertical dotted bar indicates the *GOES* flare start time, and the solid bar the extrapolated CME onset time. The average velocity of the CME front is 342 km s^{-1}, and the average acceleration is –6.2 m s^{-2}.

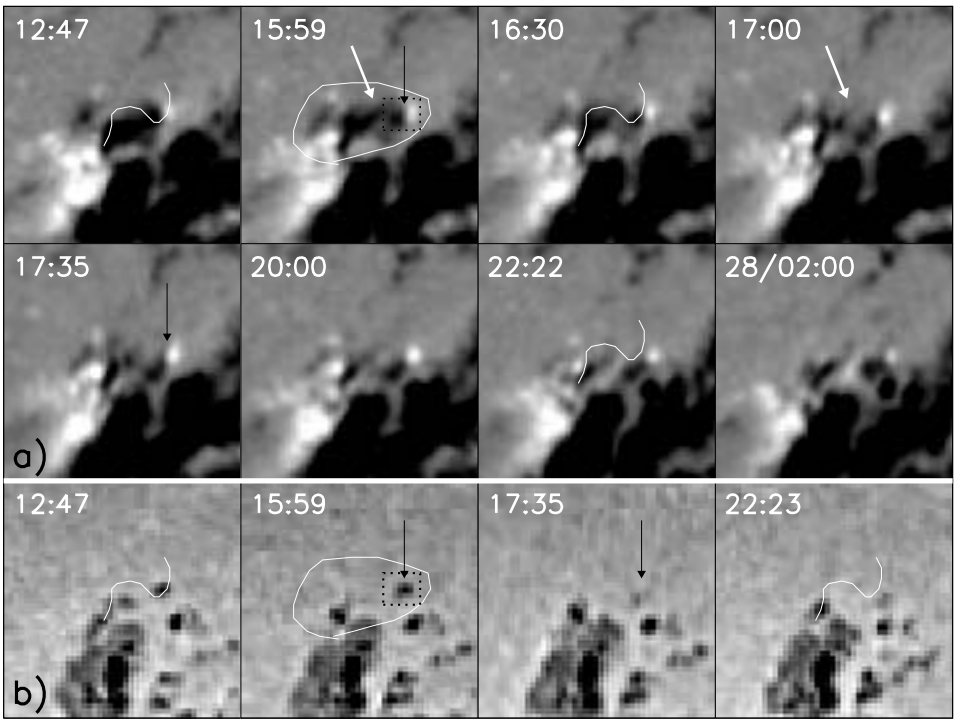

Fig. 6 MDI magnetograms (a) and continuum images (b) around the eruptive filament. The white arrows indicate the negative patch with a large reduction in area during the flare, and the black arrows the vanishing small pore. The outlines of F's axis as in Fig. 1 are plotted, and the white contours and the black boxes indicate two areas, in which the changes of magnetic flux are measured and plotted in Fig. 7. The FOV is $90'' \times 90''$. The outlines of F's axis are plotted as white curves in Fig. 6 as well as in Fig. 1. In Fig. 6, they are plotted in the images of 12:47, 16:30, 22:22 and 22:23 UT.

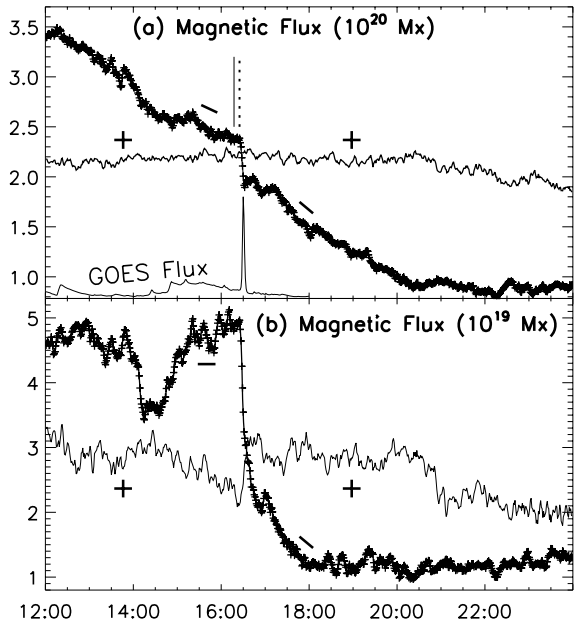

Fig. 7 Changes of magnetic flux in the contour (a) and the box (b) areas in Fig. 6, and time profiles of *GOES-8* 1–8 Å soft X-ray, which are displayed in an arbitrary unit to fit in the panel. The plus/minus sign marks the positive/negative flux. To improve clarity, the absolute values for the negative flux are plotted, and the positive flux values in panel (a) are shifted 1 on the vertical scale. The vertical dotted bar indicates the *GOES* flare start time, and the solid bar the extrapolated CME onset time.

By further examining MDI observations, we found that the F eruption was correlated with a distinct photospheric activity below it. Figure 6 shows the MDI magnetograms and continuum images around the eruptive region. At first view, it is quite clear that the area with a negative-polarity flux patch at the southern side of F greatly decreased after the eruption (indicated by the white arrows). More strikingly, a small pore just under the western part of F underwent a sudden disappearance (indicated by the black arrows). The pore was clearly seen at 15:59 UT before the eruption but it almost completely disappeared in the next available MDI intensity image at 17:35 UT. Such a disappearance thus took place in a timescale of less than 100 min. Interestingly, it showed a δ configuration by making a comparison between the 15:59 UT magnetogram and continuum image. The flux changes in an area containing the eruptive F (indicated by the white contours) and in a smaller area only including the disappearing pore (indicated by the black dotted boxes) are measured and plotted in Figure 7, and the *GOES-8* 1–8 Å soft X-ray flux profile is also overplotted to indicate the flare time. After the flare start, we see that the negative flux in the contour (box) area had an abrupt decrease on the order of 4.5×10^{19} Mx (1.7×10^{19} Mx) within the flare duration of only 7 min, i.e. it impulsively dropped about 20% (34.7%), which gives an average flux loss rate of about 1.1×10^{17} Mx s^{-1} (4.0×10^{16} Mx s^{-1}). In the following several hours, the change of the negative flux only showed a simple tendency of continuous decrease, and had no indication of a return to the pre-flare condition, indicating that such an impulsive flux loss was permanent, not transient, and thus was not due to the flare emission. We also note that the surrounding positive flux only changed a little relative to the negative flux during the flare. Therefore, the changes of opposite-polarity flux in the contour (box) area were not simultaneous and seemingly not balanced.

4 CONCLUSIONS AND DISCUSSION

By means of high-resolution observations, the event was identified as a surge-like eruption of the miniature filament F, i.e. a blowout surge, instead of a standard surge according to the following observations. (1) F divided the opposite-polarity photospheric magnetic field around the AR's northern periphery. (2) The eruption was followed by a compact, impulsive flare. In the early eruption phase, however, the initial flare brightenings had two ribbons. (3) The evolution timescales of F, from its formation to full development through eventual eruption, were similar to those in previous studies. (4) The two legs of the erupting F were spatially consistent with the two ends of the pre-eruption F. Our observations further showed that the blowout surge was closely associated with the CME along a pre-existing streamer. Therefore, these observations strongly indicated that the blowout surge, a filament eruption taking the form of a surge, was a small-scale version of the large-scale filament eruptions, with the exception of the small time and space scales (Nisticò et al. 2009; Moore et al. 2010; Raouafi et al. 2010; Hong et al. 2011).

An important aspect of the event is that, despite the very small size of F, its eruption and the following M2.2 flare were temporally and spatially relevant to a common characteristic of photospheric activity in major flares previously observed by some authors (Kosovichev & Zharkova 1999; Wang et al. 2002b; Meunier & Kosovichev 2003; Li et al. 2005, 2011; Liu et al. 2005; Sudol & Harvey 2005; Wang & Liu 2010), i.e. the sudden, significant, and persistent decrease in negative flux on the order of 4.5×10^{19} Mx and on a timescale of 7 min. As suggested by Sudol & Harvey (2005), similar changes are ubiquitous features of X-class flares and most likely resulted from changes in the magnetic field's direction rather than its strength, suggesting that they are consequences rather than the trigger of the flares. If so, the observed changes of the magnetic field in our example were probably due to the field lines being pulled or relaxed upward by the erupting F (also see Deng et al. 2005, Wang et al. 2005, and Hudson et al. 2008). As for the puzzling signature of changes of flux imbalance in two polarities, although some possible explanations were offered and discussed (Wang et al. 2002a,b; Liu et al. 2003), we also believe that it was mainly associated with such changes in the magnetic field direction. Another rare phenomenon in this example is that during the rapid flux changes a small pore nearly disappeared in less than 100 min. Only one example of Wang et al. (2002a) has demonstrated that a flare can be associated with the complete disappearance of a small sunspot in a short period, thus our event gives another clear example where a similar pore disappearance can also occur in a blowout surge.

Another key question concerning the event is why F erupted in the form of a surge. Since formation, maintenance, and instability of F should be controlled by its magnetic field environment (Martin 1990), we can tentatively consider the following three factors. First, the very small size of the F is a main element, which leads it to erupt in a narrow angular extent. We find that the erupting F showed a large rising height relative to the width between its two legs. Second, the eruption is strong enough to open its overlying coronal arcade and escape out into the heliosphere, which is indicated by the occurrence of the following flare and CME. This is clearly different from the cases observed by Wang et al. (2000), in which the most miniature erupting filaments are expelled to new locations. Note that all the miniature filaments of Wang et al. (2000) were on the quiet Sun with low magnetic flux density, while in our example F was located in a region with relatively high magnetic flux density. Therefore, it is naturally expected that a small change in the stronger magnetic field might be enough to influence the topology and stability of the F field in a violent manner and lead to a strong eruption (Gaizauskas 1989). Finally, there exists a guiding magnetic field with twofold functions to channel the F eruption and restrain its lateral swelling. The CME along the streamer suggested that the F eruption from the streamer base should be guided by its open field component. This is very similar to that occurring in standard surges, which could also be ejected along either open magnetic fields or closed large loops. It is noteworthy that, however, the physical scenarios of standard and blowout surges are different. As shown in Figure 3, magnetic reconnection only occurs between the

guiding field and the closed magnetic field of new emerging flux in the standard surge case, but in the blowout surge case reconnection might occur at different places (Moore et al. 2010). Therefore, a clear distinction between standard and blowout surges by using high-resolution observations is necessary to understand their physical natures and the origin of associated eruptive phenomena. We can imagine that if we only have Hα observations with poorer spatial resolution, the blowout surge in this example will be readily regarded as a standard one, and thus might lead to misunderstandings about the origin of the associated CME. Even though the spatial resolution of our observations is high enough, the two phenomena are so easily mistakable for each other that we should differentiate them with great care. It is anticipated that observations from the *Solar Dynamics Observatory* would be greatly beneficial in this problem.

Acknowledgements We thank an anonymous referee for many constructive suggestions and thoughtful comments that helped to improve the clarity and quality of this paper. We are grateful to the observing staff at BBSO for making good observations. We thank the *SOHO*/MDI, EIT and LASCO teams for data support. This work is supported by the National Basic Research Program of China (973 program, 2011CB811400) and by the National Natural Science Foundation of China (Grant Nos. 10973038 and 11173058).

References

Bemporad, A., Sterling, A. C., Moore, R. L., & Poletto, G. 2005, ApJ, 635, L189
Brueckner, G. E., Howard, R. A., Koomen, M. J., et al. 1995, Sol. Phys., 162, 357
Bruzek, A., & Durrant, C. J., eds. 1977, Illustrated Glossary for Solar and Solar-terrestrial Physics, Astrophysics and Space Science Library, 69 (Dordrecht: Reidel)
Canfield, R. C., Reardon, K. P., Leka, K. D., et al. 1996, ApJ, 464, 1016
Chae, J., Qiu, J., Wang, H., & Goode, P. R. 1999, ApJ, 513, L75
Chifor, C., Young, P. R., Isobe, H., et al. 2008, A&A, 481, L57
Delaboudinière, J.-P., Artzner, G. E., Brunaud, J., et al. 1995, Sol. Phys., 162, 291
Deng, N., Liu, C., Yang, G., Wang, H., & Denker, C. 2005, ApJ, 623, 1195
Dobrzycka, D., Raymond, J. C., Biesecker, D. A., Li, J., & Ciaravella, A. 2003, ApJ, 588, 586
Gaizauskas, V. 1989, Sol. Phys., 121, 135
Gilbert, H. R., Serex, E. C., Holzer, T. E., MacQueen, R. M., & McIntosh, P. S. 2001, ApJ, 550, 1093
Hermans, L. M., & Martin, S. F. 1986, in NASA Conference Publication, 2442, ed. A. I. Poland, 369
Hong, J., Jiang, Y., Zheng, R., et al. 2011, ApJ, 738, L20
Hudson, H. S., Fisher, G. H., & Welsch, B. T. 2008, in Astronomical Society of the Pacific Conference Series 383, Subsurface and Atmospheric Influences on Solar Activity, eds. R. Howe, R. W. Komm, K. S. Balasubramaniam, & G. J. D. Petrie (San Francisco: ASP), 221
Innes, D. E., Genetelli, A., Attie, R., & Potts, H. E. 2009, A&A, 495, 319
Jiang, R.-L., Shibata, K., Isobe, H., & Fang, C. 2011, RAA (Research in Astronomy and Astrophysics), 11, 701
Jiang, Y., Yang, J., Zheng, R., Bi, Y., & Yang, X. 2009, ApJ, 693, 1851
Jiang, Y. C., Chen, H. D., Li, K. J., Shen, Y. D., & Yang, L. H. 2007, A&A, 469, 331
Kahler, S. W., Moore, R. L., Kane, S. R., & Zirin, H. 1988, ApJ, 328, 824
Kosovichev, A. G., & Zharkova, V. V. 1999, Sol. Phys., 190, 45
Kurokawa, H., & Kawai, G. 1993, in IAU Colloq. 141, Astronomical Society of the Pacific Conference Series 46, The Magnetic and Velocity Fields of Solar Active Regions, eds. H. Zirin, G. Ai, & H. Wang (San Francisco: ASP), 507
Li, J. P., Ding, M. D., & Liu, Y. 2005, Sol. Phys., 229, 115
Li, Y., Jing, J., Fan, Y., & Wang, H. 2011, ApJ, 727, L19
Liu, C., Deng, N., Liu, Y., et al. 2005, ApJ, 622, 722

Liu, Y. 2008, Sol. Phys., 249, 75
Liu, Y., Jiang, Y., Ji, H., Zhang, H., & Wang, H. 2003, ApJ, 593, L137
Madjarska, M. S., Doyle, J. G., Innes, D. E., & Curdt, W. 2007, ApJ, 670, L57
Martin, S. F. 1990, in IAU Colloq. 117, Dynamics of Quiescent Prominences, 363, eds. V. Ruzdjak, & E. Tandberg-Hanssen (Berlin: Springer Verlag), 1
Meunier, N., & Kosovichev, A. 2003, A&A, 412, 541
Moore, R. L., Cirtain, J. W., Sterling, A. C., & Falconer, D. A. 2010, ApJ, 720, 757
Moore, R. L., & Sterling, A. C. 2007, ApJ, 661, 543
Moreno-Insertis, F., Galsgaard, K., & Ugarte-Urra, I. 2008, ApJ, 673, L211
Nisticò, G., Bothmer, V., Patsourakos, S., & Zimbardo, G. 2009, Sol. Phys., 259, 87
Nitta, N. V., Reames, D. V., De Rosa, M. L., et al. 2006, ApJ, 650, 438
Paraschiv, A. R., Lacatus, D. A., Badescu, T., et al. 2010, Sol. Phys., 264, 365
Pariat, E., Antiochos, S. K., & DeVore, C. R. 2010, ApJ, 714, 1762
Patsourakos, S., Pariat, E., Vourlidas, A., Antiochos, S. K., & Wuelser, J. P. 2008, ApJ, 680, L73
Petrie, G. J. D., & Sudol, J. J. 2010, ApJ, 724, 1218
Pevtsov, A. A., Balasubramaniam, K. S., & Rogers, J. W. 2003, ApJ, 595, 500
Raouafi, N.-E., Georgoulis, M. K., Rust, D. M., & Bernasconi, P. N. 2010, ApJ, 718, 981
Ren, D. B., Jiang, Y. C., Yang, J. Y., et al. 2008, Ap&SS, 318, 141
Roy, J. R. 1973, Sol. Phys., 28, 95
Sakajiri, T., Brooks, D. H., Yamamoto, T., et al. 2004, ApJ, 616, 578
Scherrer, P. H., Bogart, R. S., Bush, R. I., et al. 1995, Sol. Phys., 162, 129
Schmieder, B., Shibata, K., van Driel-Gesztelyi, L., & Freeland, S. 1995, Sol. Phys., 156, 245
Schrijver, C. J. 2010, ApJ, 710, 1480
Sheeley, N. R., Walters, J. H., Wang, Y.-M., & Howard, R. A. 1999, J. Geophys. Res., 1042, 24739
St. Cyr, O. C., Plunkett, S. P., Michels, D. J., et al. 2000, J. Geophys. Res., 105, A8, 18169
Sterling, A. C., Harra, L. K., & Moore, R. L. 2010, ApJ, 722, 1644
Sudol, J. J., & Harvey, J. W. 2005, ApJ, 635, 647
Svestka, Z., Farnik, F., & Tang, F. 1990, Sol. Phys., 127, 149
Tang, F. 1985, Sol. Phys., 102, 131
Uddin, W., Jain, R., Yoshimura, K., et al. 2004, Sol. Phys., 225, 325
Wang, H., Ji, H., Schmahl, E. J., et al. 2002a, ApJ, 580, L177
Wang, H., & Liu, C. 2010, ApJ, 716, L195
Wang, H., Liu, C., Deng, Y., & Zhang, H. 2005, ApJ, 627, 1031
Wang, H., Spirock, T. J., Qiu, J., et al. 2002b, ApJ, 576, 497
Wang, J., Li, W., Denker, C., et al. 2000, ApJ, 530, 1071
Wang, Y.-M., Pick, M., & Mason, G. M. 2006, ApJ, 639, 495
Wang, Y.-M., & Sheeley, N. R., Jr. 2002, ApJ, 575, 542
Yamauchi, Y., Wang, H., Jiang, Y., Schwadron, N., & Moore, R. L. 2005, ApJ, 629, 572
Yang, L.-H., Jiang, Y.-C., Yang, J.-Y., et al. 2011, RAA (Research in Astronomy and Astrophysics), 11, 1229
Yoshimura, K., Kurokawa, H., Shimojo, M., & Shine, R. 2003, PASJ, 55, 313
Zhang, J., Dere, K. P., Howard, R. A., Kundu, M. R., & White, S. M. 2001, ApJ, 559, 452
Zheng, R., Jiang, Y., Hong, J., et al. 2011, ApJ, 739, L39
Zuccarello, F., Battiato, V., Contarino, L., Romano, P., & Spadaro, D. 2007, A&A, 468, 299